Geomorphology 221 (2014) 124–138

Contents lists available at ScienceDirect

Geomorphology

journal homepage: www.elsevier.com/locate/geomorph

Incised relict landscapes in the eastern Alps

Nicolas Legrain [a], Kurt Stüwe [a,*], Andreas Wölfler [a,b]

[a] Institute of Earth Sciences, University of Graz, Universitätsplatz 2, 8010 Graz, Austria
[b] Institut für Geologie, Leibniz Universität, Callinstraße 30, D-30167 Hannover, Germany

ARTICLE INFO

Article history:
Received 4 June 2013
Received in revised form 5 June 2014
Accepted 8 June 2014
Available online 19 June 2014

Keywords:
Channel profiles
Relict landscape
Low-temperature thermochronology
Eastern Alps
Landscape evolution

ABSTRACT

We investigate landscape evolution in a region of the Alps that has escaped glacial erosion during periodic glaciations of the last million years. The research is thus suited to investigate landscaping processes on a longer time scale at the eastern end of the Alps. Morphometric analysis reveals the presence of incised relict landscapes in several regions. In the Koralpe range topographic analysis is interpreted in terms of the relict landscape being present on both sides of the eastward tilted Koralpe block. This suggests that the relict landscape is younger than the tilting of the range, which is inferred to have taken place between 18 and 16 Ma. In the Pohorje region, a relict landscape is developed across the contacts of a 19 Ma pluton. We use apatite (U–Th)/He thermochronology to constrain the possible age of the Koralpe and Pohorje relict landscapes. The results indicate that the Pohorje massif had cooled below 70 °C by about 15 Ma suggesting that the relict landscape must be younger — consistent with the interpretation of the Koralpe range. These results suggest that many relict landscapes of the eastern Alps may have formed after 15 Ma in a period of tectonic quiescence and erosion. However, in both ranges channel profile projections show that about 387 ± 105 m uplift and incision occurred subsequently. This incision is likely to have occurred during the last 6–5 Ma in response to the uplift of the whole region. It testifies to a renewed and ongoing uplift event that is earlier than the glaciation periods but might easily be confused with impact of glacial erosion elsewhere in the eastern Alps.

1. Introduction

Topography is the result of a competition between erosion that removes material from the Earth's surface, and tectonic forces that can create relief through uplift mechanisms. The interaction and competition between these different forces that shape the morphology of mountain belts is a topical subject in modern geoscience. In particular in the European Alps, the debate on landscape evolution and its relationship with tectonics and climate remains ongoing (Cederbom et al., 2004; Persaud and Pfiffner, 2004; Champagnac et al., 2007; Hergarten et al., 2010; Norton et al., 2010; Willett, 2010; Valla et al., 2011; Sternai et al., 2012). Here aspects of the long-term landscape evolution of the Alps are inferred by focusing on a part of the eastern Alps that was free of ice during the last periodic glaciations (van Husen, 1997), but features a mountainous landscape with summits up to 2200 m surface elevation: the easternmost part of the eastern Alps (Fig. 1). As this region was not affected by glacial scour, it represents an excellent opportunity to document the landscape evolution of the area on a time scale that reaches substantially further back than the periods of glaciation.

Paleosurfaces or relict landscapes have long been documented in the studied area, in particular for the Koralpe Mountain (Fig. 1). Winkler-Hermaden (1957) already suggested that the Koralpe Mountain features preserved 'paleosurfaces', or relict landscapes as we term these landforms here. More recently, the Koralpe landscape has been considered as an Oligocene paleosurface by Frisch et al. (2000). Robl et al. (2008) have also suspected that knickpoints may be recorded in the river profiles of some of the tributaries of the Drava and the Mur draining the Koralpe and Pohorje mountains, possibly indicating transient erosion. However, the Koralpe and Pohorje landforms were never mapped using quantitative methods and digital elevation models (DEM) and the age of their formation and incision remains largely unconstrained (although see: Rantitsch et al., 2009). To investigate the landscape evolution, the uplift history and the links with tectonic events in this part of the Alps, channel profiles and slope maps were analyzed to derive maps of incised relict landscapes for the Koralpe and Pohorje mountains. Channel profile projections of eight selected rivers were then used to estimate the amount of incision into these relict landscapes. We combine our results with 20 new apatite (U–Th)/He ages from the Koralpe and Pohorje mountains that are used to constrain the interpretations in absolute time. Finally, an integrated landscape evolution scenario is inferred for the studied area linking tectonic and landscape evolution of the region since the early Miocene.

2. Geological setting

The Pohorje Massif and the Koralpe region are both part of what has been termed the Styrian Block, which encompasses the entire region

* Corresponding author. Tel.: +43 3163805682.
E-mail address: kurt.stuewe@uni-graz.at (K. Stüwe).

http://dx.doi.org/10.1016/j.geomorph.2014.06.010
0169-555X/

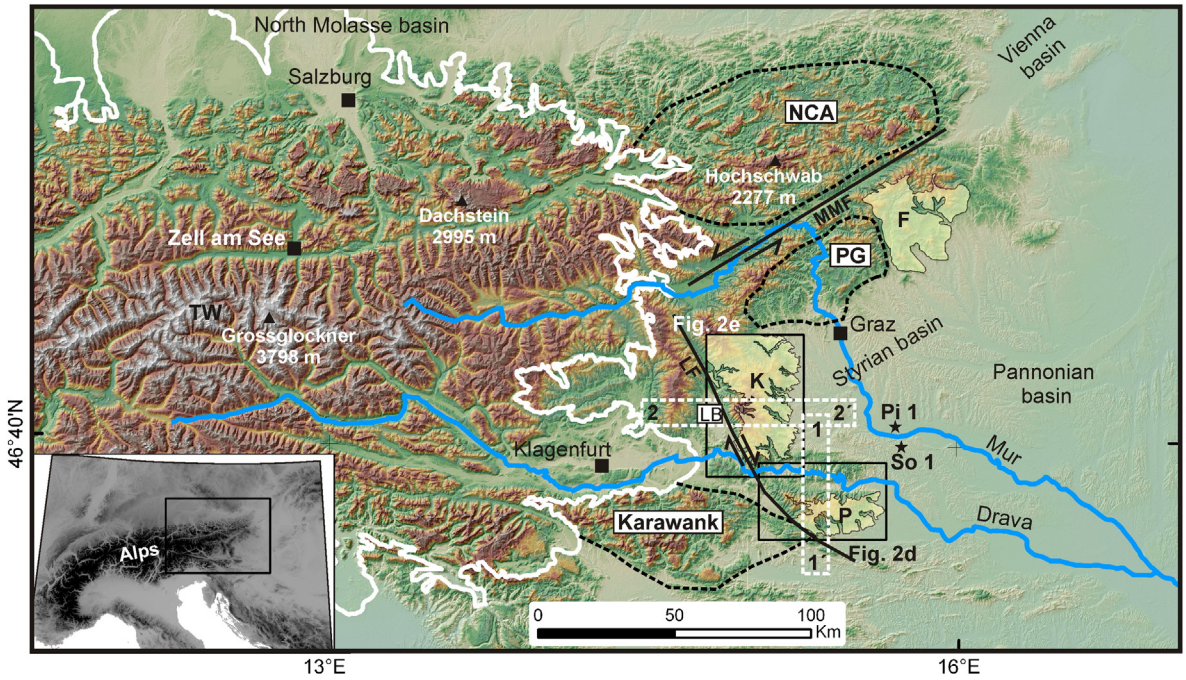

Fig. 1. Topography of the easternmost part of the European Alps and location of the studied areas. Thick white line represents limit of glaciation during the glaciation periods. Relict landscapes outside this region are shown as shaded regions. NCA = Northern Calcareous Alps; TW = Tauern window; PG = Paleozoic of Graz; K = Koralpe relict landscape; P = Pohorje relict landscape; LB = Lavanttal basin; LF = Lavanttal fault; MMF = Mur-Mürz fault. F refers to the Fischbacher Mountain that also represents an incised relict landscape. Location of wells for subsidence analysis: So 1: Somat 1; Pi 1: Pichla 1 (Ebner and Sachsenhofer, 1995; Sachsenhofer et al., 1998, 2001). White dashed rectangles are extent of swath profiles of Fig. 4 (profiles 1–1′ and 2–2′).

east of the Lavanttal fault system and south of the Mur-Mürz system including the Styrian basin (Fig. 1) (Wagner et al., 2011). The Lavanttal fault system and the Mur-Mürz systems are both some of the major structures controlling the Miocene lateral extrusion of the eastern Alps (Ratschbacher et al., 1991; Frisch et al., 1998; Robl and Stüwe, 2005; Wölfler et al., 2010, 2011) and are therefore closely linked to the tectonic evolution of the region (Fig. 1). The regional base level for the entire eastern end of the Alps is set by the Danube which ultimately drains into the Black Sea. More locally, the current base levels for the region under investigation are the Drava and the Mur rivers (Fig. 1). These two major rivers seem to be morphologically well-equilibrated and do not record significant knickpoints other than the ones located at the LGM terminal moraines (Robl et al., 2008). The Styrian basin consists of sediments that were deposited between approximately 18 and 7 Ma (Ebner and Sachsenhofer, 1995). This region is characterized by a smooth hilly landscape and extensive alluvial plains and fluvial terraces (e.g. Wagner et al., 2011).

The Pohorje Massif lies at the southeastern corner of the Alps (Fig. 1). The massif is about 35 km long and 15 km wide and it is surrounded by the westernmost parts of the Pannonian basin to the south and to the east. The elevation of the Miocene basin to the south is about 300 m and the highest summit of Pohorje is Črni Vrh with an elevation of 1543 m. The massif is made up of eclogite facies Cretaceous paragneisses of the Austroalpine nappe complex. The metamorphic rocks of the Pohorje Mountain were intruded by the Pohorje pluton, a 30 km-long and 4-8 km-wide magmatic body (Fig. 2d). U–Pb analysis on zircons implies an early Miocene crystallization age of the granite around 19 Ma and zircon fission track ages indicate rapid cooling of the pluton within about 3 Ma (Fodor et al., 2008). However, cooling and exhumation of Pohorje pluton below about 250 °C are currently unconstrained. However, detrital apatite fission track ages indicate that the pluton supplied already in the middle Miocene sediments into the Ribnica Trough in the center of the massif — (Sachsenhofer et al., 1997, 1998; Dunkl et al., 2005). This is supported by kinematic data from east–west striking, high-angle normal faults along the margin of the Ribnica Trough (Pischinger et al., 2008). Also, associated volcanic rocks at the western end of the massif indicate that the pluton cooled near the surface. Sölva et al. (2005) have noted that the course of the Drava river that dissects the massif indicates an antecedent river profile with young uplift of the massif.

The Koralpe region is a north–south striking range located between the Styrian basin to the east and the Miocene Lavanttal fault to the west (Figs. 1, 2e). The range measures ~40 km from north to south and ~25 km from east to west. It has an asymmetric topography from 2140 m on the Speikkogel summit to 300 m near the Styrian basin with a steep western slope and a gentle eastern slope, probably due to tilting of the range in response to the lateral extrusion of the eastern Alps and the early Miocene fault activity of the Lavanttal fault (Neubauer and Genser, 1990; Kurz et al., 2011). Lithologically, the range is famous for hosting the eclogite type locality and is one of the highest grade metamorphic regions of the Alps. It is made up of Cretaceous gneisses, amphibolites and eclogites. The Miocene Lavanttal fault system bounding the range to the west is part of the Pöls-Lavanttal fault system (Fig. 2e) that has a dextral offset (Exner, 1976; Wölfler et al., 2010, 2011). In the Lavanttal segment, a small pull-apart basin shows evidence for about 15 km of dextral offset (Reischenbacher et al., 2007). Vertical offset along the Lavanttal fault system is estimated to be >2 km, with relative upward movement of the Koralpe (Frisch et al., 2000). Onset of sedimentation in the Lavanttal basin is dated to ~18 Ma (Strauss et al., 2001; Reischenbacher et al., 2007). Based on the sedimentary evolution of the basin, the Lavanttal fault system is assumed to be active since the early Miocene, with peaks in activity at 18–16 and 14–12 Ma (Reischenbacher et al., 2007; Wölfler et al., 2010). Fault plane solutions for recent seismicity display dextral strike-slip movements (Reinecker and Lenhardt, 1999; Pischinger et al., 2008). The Koralpe Mountain was partly covered by small isolated glaciers during the recent glaciation periods. These glaciers have left small cirques around the highest peaks, but the glaciers only covered and modified a very small part of the Koralpe landscape (Fig. 2d) that we exclude from the geomorphic analysis.

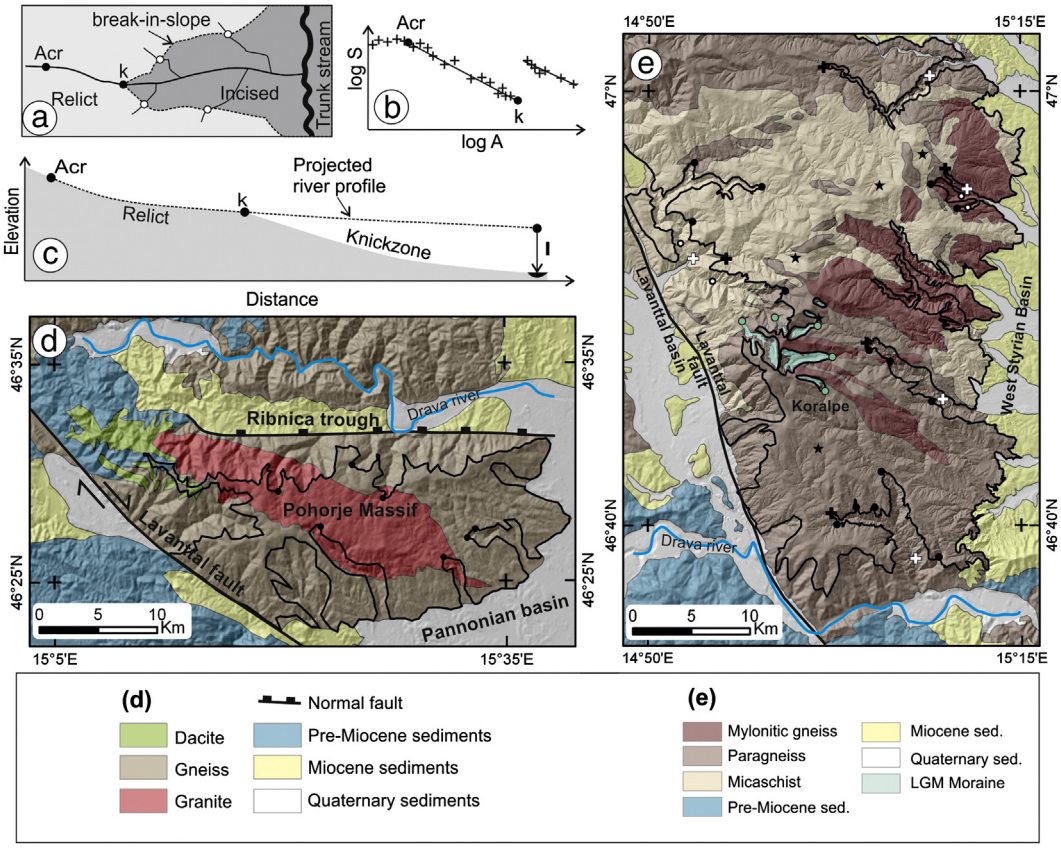

Fig. 2. Lithologies, geomorphology and mapped separation line of relict and incised landscapes for the Koralpe and Pohorje regions as well as the method for mapping the incised relict landscape and projecting channel profiles. (a)–(c) Conceptual model for the use of the mapping. (a) Map view of a relict and incised landscape, white points are the location of knickpoints of tributaries; Points along river are: Acr: critical drainage area above which log (S) and log (A) start to be correlated; k: knickpoint. (b) Double logarithmic slope-area plot with fitted relict and knickzone segments; $S =$ gradient in m/m; $A =$ Drainage area in m^2. (c) River profile with the downstream projected relict river segment; I is the incision calculated at the confluence with the trunk stream. For the rivers draining to Miocene basins, the incision was calculated at the transition between crystalline basement and basin. (d) Map of the Pohorje Mountain showing the extent of the relict landscape (black line) and lithology. (e) Map of the Koralpe Mountain, showing the mapped relict landscape (black line) and the lithology, for more details on other symbols refer to Fig. 3.

3. Methods

In order to constrain relict and incised landscapes and the amount of uplift that separates the two as well as the timing of this uplift, we have used quantitative methods now well established as tools for the interpretation of fluvially-sculpted landscapes as well as low-temperature thermochronological methods for absolute dating. As the thermochronological method, (U–Th)/He dating of apatite is selected because this system has the lowest closure temperature of the well-established thermochronological systems. It can thus be used as a proxy for landscape evolution. Details of the methods are discussed separately.

3.1. Mapping of incised and relict landscape

Here the terms "relict landscape" and "incised landscape" are used in their most simple definitions (see Fig. 2a–c), referring to the concept of an incision of rivers into a pre-existing morphology resulting in two different landscapes: the pre-existing "relict" landscape and the more recent "incised" landscape (Clark et al., 2006). The morphometric analysis was performed by using the SRTM3 digital elevation model (DEM). Although a 30 m resolution DEM exists (ASTER 30 m), a recent study suggests that, at the moment, the available version of the 30 m DEM is less accurate than the SRTM3 data with about 90 m resolution (Hirt et al., 2010). This was confirmed here by performing a preliminary comparison of the two DEMs for some of the studied rivers. Channels were studied by using the empirical relationship between drainage area A and slope S of an equilibrated channel (Hack, 1973; Flint, 1974):

$$S = k_s A^{-\theta}$$

where θ and k_s are generally referred to as the concavity index and the channel steepness index, respectively (Wobus et al., 2006).

The data for A and S were extracted from the DEM by using the methods of Wobus et al. (2006) and the freely available Stream Profiler codes (Whipple et al., 2007). Because k_s is strongly related to θ, a normalized channel steepness index (k_{sn}) is often calculated using a fixed reference concavity index (θ_{ref}). This allows for easier comparison between different channels or different channel segments. If the channel is considered to be in equilibrium (for example because they have no knickpoints along the channel — see below), only single values of θ and k_s should be fitted in a doubly logarithmic slope-area plot (Fig. 2b). Then, k_{sn} can be used as a proxy to infer information on rock uplift rates (Wobus et al., 2006). This can be illustrated by listing another definition of the steepness index where:

$$k_s = (U/K)^{1/n}$$

and U is the uplift rate and K and n are the constants related to the material properties. The two equations above can be related and the interested reader is referred to Wobus et al. (2006) for their relationship.

If the channel is not in equilibrium, channel profiles will depart from the shape implied by the equations above. Thus, these relationships

can also be used to identify different segments of the river profiles (Fig. 2a–c). Then, the fit must be done separately for the different segments of the channel. Here we use this latter approach as all channel profiles presented here have marked knickzones, defined as a steep channel segment bound by less steep channel reaches. The uppermost point of the knickzone is defined as a knickpoint *k*. Interpretation of knickpoints or knickzones is not trivial as they may be controlled by either lithological boundaries or tectonic and climatic controls. As our interest is predominantly in tectonically and climatically related knickpoints, we have carefully compared the location of knickzones with lithological maps. Maps of normalized channel steepness index were calculated using a reference concavity index $\theta_{ref} = 0.45$ which is the most commonly used value in the literature (Fig. 3a,c; Wobus et al., 2006). This allows for easier direct comparison with recent studies. Note that the choice of θ_{ref} does not change the relative pattern of k_{sn}.

The incised valleys were mapped by following obvious breaks-in-slope based on the slope maps and the k_{sn} maps (Figs. 2, 3). The incised landscape is recognized by significantly higher slope and higher k_{sn} values than the surrounding relict landscape (Fig. 3a). The mapping of relict and incised landscapes was based on the DEM analysis and cross-checked with field observations. Field work consisted of comparing the bedrock versus alluvial parts of the channels as well as the soil thickness in the incised part of the landscape and on the relict landscape. Bedrock or mixed bedrock-alluvial channels in the incised parts

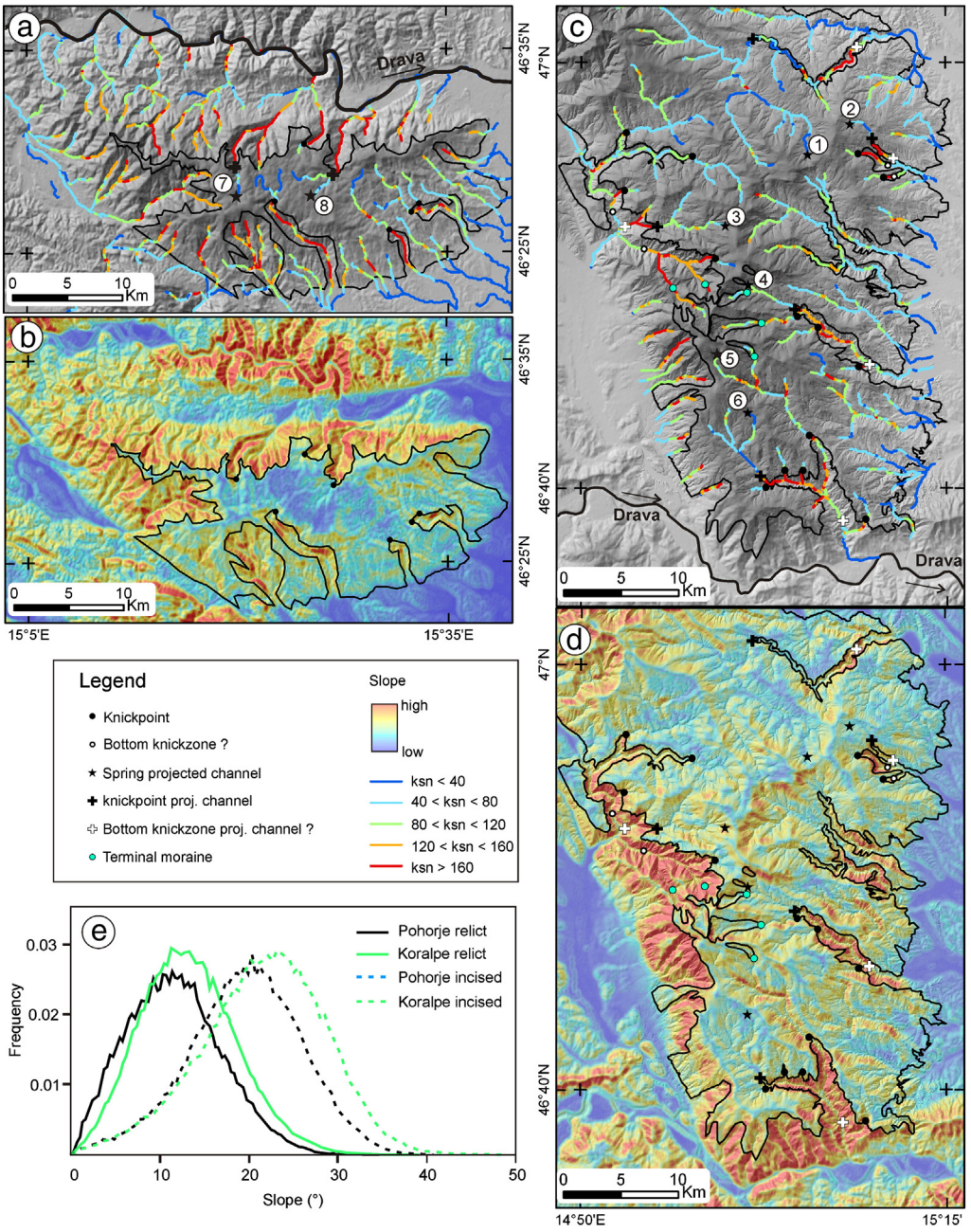

Fig. 3. Mapping results for the Pohorje Massif in northern Slovenia and Koralpe regions, (a) and (c): Maps of normalized channel steepness index (*ksn*) for Koralpe and Pohorje regions, calculated with a reference concavity index of 0.45 and with 500 m segments along all channels with $A > 106$ m^2. Black line is the contour of the mapped relict landscape. Numbers refer to the projected channel profiles shown in Figs. 6 and 7: 1 = Waldensteinerbach: 2 = Fallegbach; 3 = Frassbach; 4 = Schwarze Sulm; 5 = Krennbach; 6 = Feistritz; 7 = Rodoljna; 8 = Lobnica. (b) and (d): Slope maps of Pohorje and Koralpe regions, calculated from the 90 m SRTM3 data. Black line is the contour of the mapped relict landscape. The LGM small glacier is excluded from the relict landscape (see also Fig. 2). (e) Slope distribution of the Koralpe and Pohorje relict and incised landscapes. The slope distribution of the Pohorje and Koralpe relict landscapes is very similar as well as the slope distribution of the two incised landscapes.

of a landscape are a good indication of relatively active incision, while alluvial channels were often observed in the relict landscape and indicate a rather low channel erosion process.

3.2. Channel profiles projection

The amount of incision into a relict landscape can be estimated by projecting "relict" river segments (Schoenbohm et al., 2004; Clark et al., 2005). This method commonly uses a fixed reference concavity index (θ_{ref}) to calculate the steepness index and then extrapolate the relict channel profile downstream. The amount of incision is then taken as the vertical difference between the extrapolated and the present day channel profile (Fig. 2c) and is interpreted as the amount of surface uplift of the range relative to base level. The reference concavity index is usually taken as the average value of the concavity indices observed in the relict river segments from a sufficient number of rivers. This approach is thus relevant for studying large areas where many channels are present. Here, only approximately 20 main rivers are present for the Koralpe and Pohorje mountains because the studied region is small. Of these 20 channels, eight were found to be suitable for downstream projection. For the other channels, the incision wave has migrated to far upstream and the remaining relict segment is too small to be reliably projected downstream. This is due to the fact that the relict landscapes in the investigated regions are not peneplains, but in themselves bear about 1000 m relief (between 1000 m and more than 2000 m surface elevation) including low, high, steep and shallower channels. However, our choice of only eight rivers of approximately 20 does not bring into doubt the interpretation of an incised relict landscape for the entire Pohorje and Koralpe mountains, as it can be clearly seen at the scale of the entire area on Fig. 3. To ensure a reliable and unambiguous downstream projection, the 8 channels were chosen based on conservative arguments on the robustness of their fit in the slope-area plots.

We used θ and k_s values given by the best fit of the relict (upper) river segment of each individual river (Fig. 2). The relict river segment was defined between the minimum critical drainage area A_{cr} in the headwaters of a channel (where $log\,(S)$ and $log\,(A)$ start to become correlated, Fig. 2a–c) and the top of the knickpoint k. The relict portion of the river was then projected downstream using the θ and k_s values of the upper relict segment. For the channels draining directly into the Drava river-, (which represent the regional base level for the entire region studied here and is a well equilibrated channel so that we interpret it as antecedent, i.e. that it remained at base level at all times of uplift; Robl et al., 2008), the relict segment was projected to the confluence with the Drava river. The derived amount of incision I refers to the vertical difference between the extrapolated and present-day profile at this particular point (Fig. 2c). For the channels draining toward Miocene basins, we have projected the channel profiles to the transition between crystalline basement and basin because we cannot assume similar concavity and steepness indices for the two areas due to their different lithology. For these rivers the incision I refers to the vertical difference between projected and present-day channel profile at the transition between crystalline basement and basin sediments.

3.3. Apatite (U–Th)/He-thermochronology

Apatite (U–Th)/He-thermochronology is useful for reconstructing the thermal history of the upper crust and may be used as a proxy to infer the morphological evolution of the Earth's surface (e.g. Ehlers and Farley, 2003). The closure temperature of this system ranges between 55 °C and 70 °C, depending on grain size, cooling rate and radiation damage (e.g. Farley, 2000; Ehlers and Farley, 2003; Shuster et al., 2006), but the method is sensitive in the temperature range between approximately 80 °C and 40 °C (Wolf et al., 1998), an interval that is called the Partial Retention Zone. Depending on the geothermal gradient (typically between 25 °C/km and 40 °C/km), apatite (U–Th)/He-thermochronology can record exhumation of rocks from about 1 to 4 km depth. We analyzed single-grain aliquots and measured at least one duplicate of every sample. The reported sample age is the mean of the single grain ages with the standard deviation as 1σ error. Six replicate analyses of Durango apatite yielded a mean age of 32.6 ± 1.5 Ma, which is in good agreement with the Durango apatite reference age of 31.44 ± 0.18 Ma (McDowell et al., 2005). Sample processing and He measurements were measured at the University of Tübingen. U, Th and Sm concentrations have been measured at the University of Arizona.

4. Results

Using the methods discussed above, the incised relict landscapes have been mapped in the two selected key regions. For the Pohorje Massif, the results are summarized in Fig. 3a,b. The black line separating the relict from the incised landscape on Fig. 3 was mapped following the boundary of the low slope area (Fig. 3a) compared to the steeper incised landscape and using a combination of interpreting local slope, relief k_{sn} patterns and knickpoint locations. The highest elevation of the mapped relict landscape is the summit of the Pohorje Mountain (1543 m) and the lowest elevation is about 300 m in the southern part of the range, at the boundary with the Pannonian basin. No relationship can be seen between the extent of the incised and relict landscape with the boundary of the granite pluton (Figs. 3b, 4d). We conclude that the incised relict landscape of Pohorje is not related to lithology. The k_{sn} map (Fig. 3a) shows a similar situation to the hillslopes, with low k_{sn} values on the relict landscape and higher values for the incised landscape. The mapping results for the Koralpe region are shown in Fig. 3c, d. The mapped relict landscape includes most of the Koralpe topography and its summit, the Speikkogel (2140 m). The lowest elevation of the mapped relict landscape is about 350 m at the eastern boundary of Koralpe. As such, it is important to note that there is more than 1000 m of relief on the relict landscape, making it difficult to separate relict and incised landscapes simply on the basis of slope. In other words, relict and incised landscapes do not correspond to a "high relict plateau" dissected by "steeply incised channels" of the younger landscape, so that mapping of their separation is difficult and unclear in many places. Nevertheless, much of the range is considered to be part of the relict landscape (even at reasonably low elevations) and only small areas in the catchments of the rivers, and their steep gorges are part of the newly incised landscape. Clearly, these incised landforms are easiest to recognize in regions where the old relict landscape is at higher elevations. The relief map (Fig. 3b) and the k_{sn} map (Fig. 3a) match well and show a well-preserved incised relict landscape. In the Pohorje massif the situation is similar: there is no relationship between the relict landscape boundary and the lithology (Fig. 4b). The slope distribution of the mapped relict landscapes display similar pattern for Koralpe and Pohorje (Fig. 3e) with an average slope of 13° and 12°, respectively. Both the Koralpe and Pohorje relict landscape slope distributions are skewed toward low values (0.3), which indicate a predominance of low-over steep slopes. Koralpe and Pohorje incised landscapes average 21° and 19°-, respectively, with a slight skewness toward high slopes (−0.2). The slope distribution shows that both areas display very similar morphometric patterns despite their different lithologies and exhumation history. The asymmetry of the Koralpe range is clearly visible on Fig. 4, with a steep western slope facing the Lavanttal basin and a gentle eastern slope facing the Styrian basin. Photographs of the mapped incised relict landscapes for the Pohorje and Koralpe regions are shown in Fig. 5.

4.1. Quantification of the amount of incision

In order to quantify the amount of incision into the Koralpe and Pohorje landscape the projection method described above was used. Four of the eight selected channels drain the Koralpe range toward the

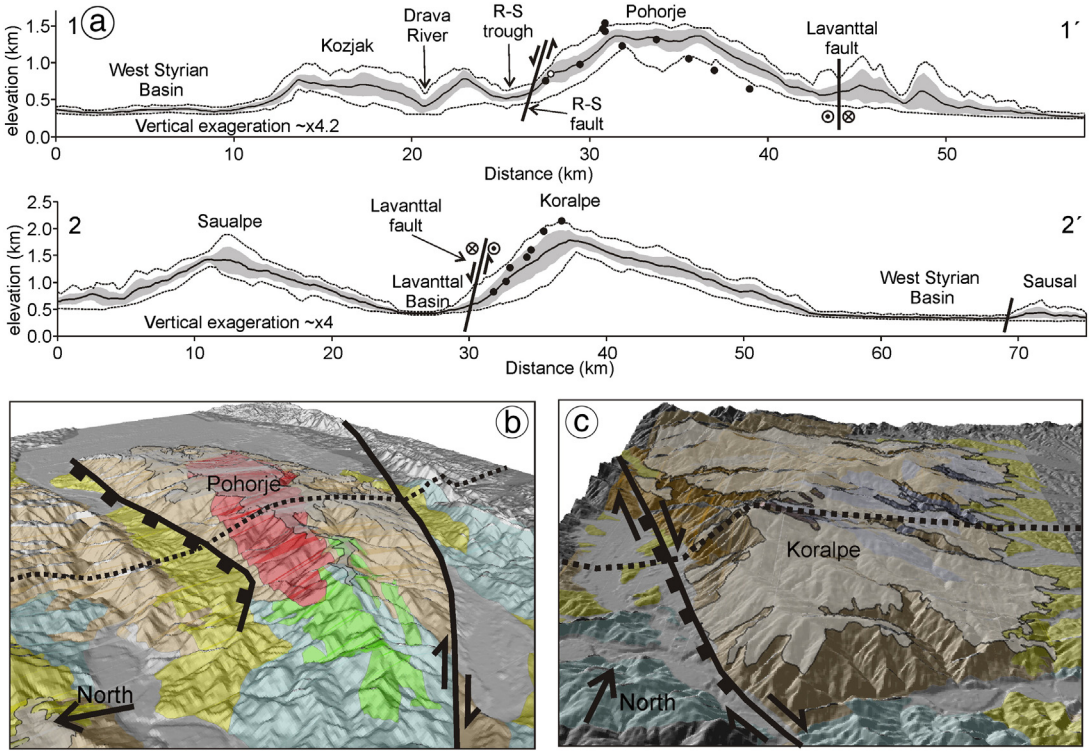

Fig. 4. Swath profiles and oblique views of the Koralpe and Pohorje mountains. (a) Swath profiles of Pohorje (1–1′) and Koralpe (2–2′); for location of the swaths see Fig. 1; Solid black line is the mean elevation, gray area is the standard deviation and dashed lines are the minimum and maximum elevations. Black and white points represent the locations of samples for apatite (U–Th)/He thermochronology, or their projection when they are located outside of the swath. On the Pohorje profile, the white point refers to the sample P2 which is a volcanic dyke; all other samples are from the granite; R–S: Ribnica–Selnica. (c) Oblique view of Pohorje from the northwest showing lithologies and morphology. Gray transparent polygon is the mapped relict landscape. The cross-cutting relationship between the granite and the relict landscape is well visible. Dashed line represents approximately the trace of the swath profile. (d) Oblique view of Koralpe from the south. Gray transparent polygon is the mapped relict landscape. Dashed line represents approximately the trace of the swath profile.

Miocene basins: the Waldensteinerbach (channel 1), the Fallegbach (channel 2) and the Schwarze Sulm (channel 4) that drain into the Styrian basin in the east before joining the Mur river, and the Frassbach (channel 3) that drains to the Lavanttal basin in the west before joining the Drava river (Fig. 6). The other four selected channels drain directly into the Drava river (Fig. 7) and are: the Radoljna river (channel 7) and the Lobnica river (channel 8) from the Pohorje range, the Krennbach river (channel 5) and the Feistritz river (channel 6) from Koralpe. The calculated amount of incision ranges from 216 to 527 m, with an average of 387 ± 105 m for the eight investigated rivers (Table 1). The calculated amount for the two Pohorje rivers is slightly higher than that for the Koralpe channels. However, due to the large uncertainty of the Pohorje incision, the amounts of incision in the two regions cannot be distinguished and they are therefore discussed together. Whether the incision is related to surface uplift of the Koralpe and Pohorje mountains or to incision of a previously elevated landscape will be discussed below.

4.2. Time constraints on the formation of the relict landscapes

The results of the channel projections have shown that only several hundreds of meters (~400 m) have been incised in the two studied regions, which are not enough to be recorded by apatite (U–Th)/He-thermochronology. However, apatite (U–Th)/He can provide time constraints on the formation of the relict landscapes prior to the incision and, importantly, the link between the relict landscapes and the active faulting that took place during the Early Miocene in the frame of the lateral extrusion of the eastern Alps. In other words, we aim to determine whether: (1) the relict landscape formed before the early Miocene faulting and, thus, represents a deformed landscape that can be used as a passive marker for deformation and uplift, or: (2) if the relict landscape formed after the early Miocene faulting and is not a deformed surface.

In order to solve this question we have collected in total 20 samples from Koralpe and Pohorje ranges (Fig. 8; Tables 2, 3). From Koralpe, nine samples were analyzed. The western slope of Koralpe is directly facing the Lavanttal fault (Figs. 4, 8) and the samples KOR1 to KOR7 were taken to form an age–elevation profile from the Koralpe summit at 2140 m elevation down toward the Lavanttal valley at 1015 m elevation (Figs. 4b, 8). In addition, two more samples (one from high elevation, and one from low elevation) where taken from a transect further south, plus one sample from further north in the Koralpe region. In general, the apatite (U–Th)/He ages range between 21.4 ± 6.2 Ma and 34.3 ± 1.5 Ma (Tables 2, 3, Fig. 8). The relationship between the apatite (U–Th)/He ages and sample elevation can be used to estimate exhumation rates. The samples from the western slope show a moderate linear fit ($r^2 = 0.54$), with an inferred exhumation rate of 105 m/my from 31 to 21 Ma (Fig. 9a). This exhumation rate is very similar to the one documented from apatite fission track data obtained by Hejl (1997) (82 m/my) indicating a steady exhumation history of about 100 m/my from the Eocene into the early Miocene. This indicates that the Koralpe has experienced very little exhumation during the whole Miocene and the apatite (U–Th)/He ages were apparently not affected by the tectonically very active early Miocene period (18 to 16 Ma).

10 apatite ages were measured from the Pohorje Mountain region. Nine samples were taken from the granite, and one from a volcanic dyke of dacite (Fig. 8, sample P2). The apatite (U–Th)/He ages from the granite range between 20.4 ± 2.5 Ma and 18.9 ± 1.9 Ma, while the age of the volcanic dyke is younger (13.9 ± 2.3 Ma). The ages do not correlate with elevation, suggesting that the samples cooled rapidly

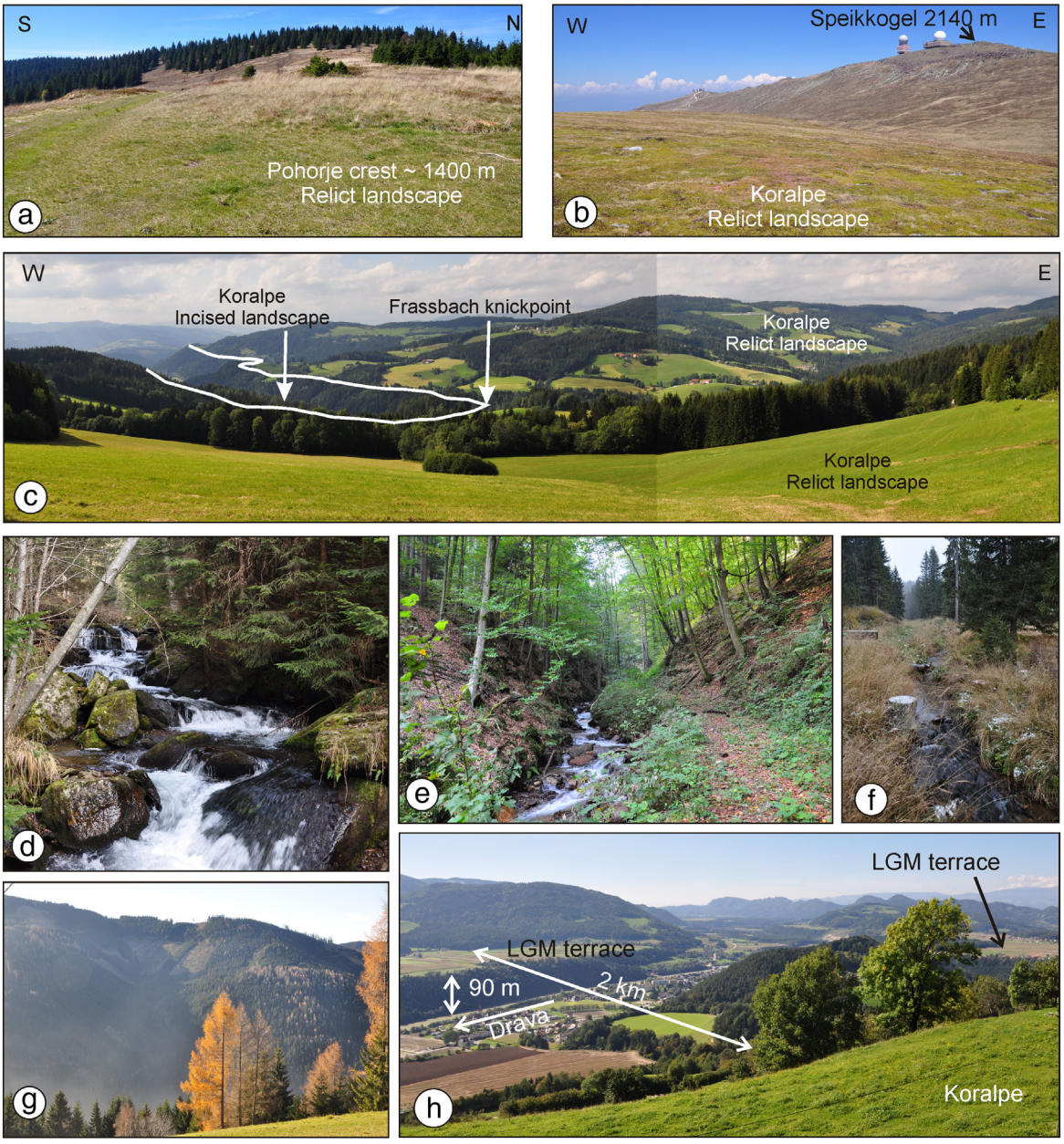

Fig. 5. Photographs of the investigated regions and their incised relict landscapes. (a) View of the very smooth crest of Pohorje forming part of the relict landscape. (b) View from the southwest of the Koralpe summit (Speikkogel). This side of the Koralpe summit was not affected by LGM glacier carving and the small glacier cirques are located on the northeast side of the summit, behind the crest in the background. (c) View to the north of the Frassbach catchment and knickpoint (projected river channel number 3), white line is the break-in-slope between the relict and incised landscape. (d) View looking upstream of the Prössingbach river (located to the south of the Frassbach river) in the incised landscape. The channel features many small waterfalls and bedrock outcrops are visible. (e) Steep hillslopes in the Koralpe incised landscape. (f) View looking upstream of the Prössingbach river on the relict landscape (compare to Fig. 5d), the river is flowing on its own deposits (alluvial) and no bedrock outcrop in the channel is present. (g) View to the south, from the crest between Prössingbach and Frassbach, into the Prössingbach incised valley showing the steep hillslopes of the incised landscape; and (h) View to the northwest from Koralpe of the Drava river LGM terraces in the last visible part of the Drava valley in the background is the terminal moraine from LGM.

below 55–70 °C by ~15 Ma (Fig. 9). The ages from the granitic samples are highly homogeneous and suggest that all samples had cooled down below 70 °C by ~15 Ma. The Pohorje pluton probably intruded the Austroalpine unit at a very shallow level where ambient temperatures were below 70 °C. However, the apparent very fast exhumation of the granite cannot be only related to cooling due to crystallization of the magma into granite because granitic pebbles have been found in 17 Ma old sediments in the adjacent sedimentary basins (Fodor et al., 2008). So at least a part of this fast cooling is related to exhumation (i.e. movement toward the surface) instead of ambient cooling because some parts of the pluton were already at the surface by 17 Ma (Fig. 9). As already interpreted by Sachsenhofer et al. (1998), and considering the tectonic context of the Pohorje Mountain (Fig. 3), this very fast exhumation is probably more due to tectonic denudation from normal faulting of the Ribnica Fault, rather than to erosion. Regardless of the relative proportion of erosion and tectonic denudation, and considering that the relict landscape of Pohorje is developed onto and crosscuts the granite, it can be interpreted that the relict landscape is younger than the granite. Thus, our ages from the Pohorje region give an upper bound for the formation of the relict landscape that cannot be older than about 15 Ma as constrained by the apatite fission track data of Fodor et al. (2008) and the data presented here (Fig. 9b).

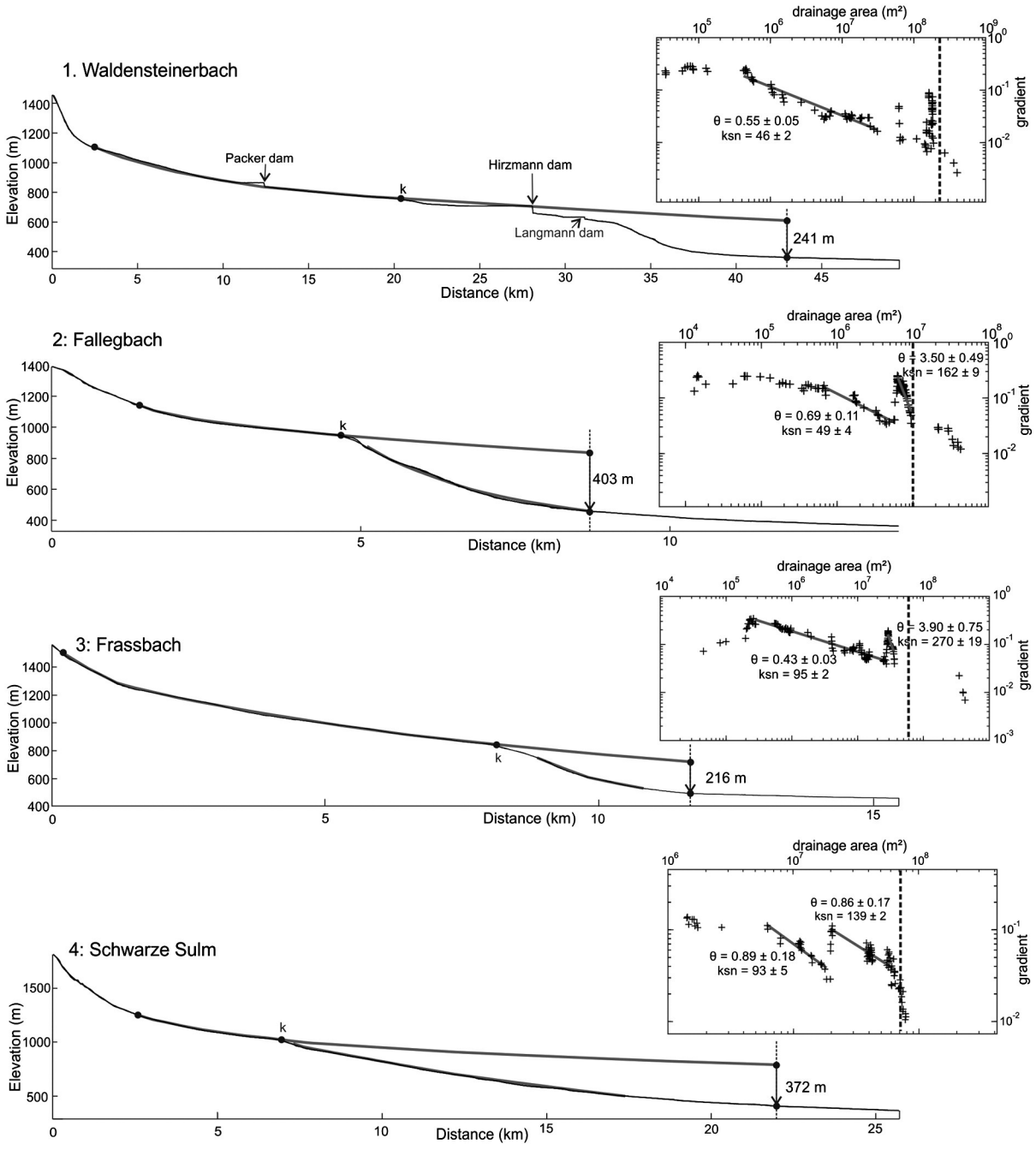

Fig. 6. Channel profile projection for the four selected channels of Koralpe draining to Miocene Basins. For location of the channels refer to Fig. 3. Thin black lines are the raw and the smoothed channel profiles, thick gray lines are the fitted segments; k = knickpoint. The vertical dashed lines in the insets of the different plots are the location of the transition between crystalline basement and basin where the incision amount is calculated. For detailed method and parameters used for the slope-area plots refer to Table 1.

5. Discussion

In the following section an integrated landscape evolution scenario is inferred for the south eastern corner of the Alps since the early Miocene. The inferred scenario is based on different data sets that include: (1) our morphometric analysis and our new apatite (U–Th)/He ages, (2) existing low-temperature thermochronological ages and, (3) existing subsidence analysis of the Miocene basins. This inferred scenario is summarized in Fig. 10. Our apatite (U–Th)/He ages show that, by 18 Ma, the Pohorje pluton was not yet exhumed and can be used as an upper bound for the creation of the relict landscape (Fig. 10). For the Koralpe landscape, the ages cannot directly give constraints on the relict landscape formation timing. The Koralpe range has been considered as an eastward tilted block (Neubauer and Genser, 1990) and the asymmetry of the range is nicely visible on Fig. 3. In this context, if the relict landscape were older than the tilting, the relict landscape should only be present on the eastern slope of Koralpe. However, the morphometric analysis has revealed that the Koralpe relict landscape is not only developed on the eastern gentle slope but more or less at similar elevations on both sides of the range (Figs. 3, 4). While equilibrated channel segments occur both above and below the relict landscape, it seems clear that the shape of the relict landscape does not reflect the overall morphological asymmetry of the range. This suggests that the formation of the Koralpe relict landscape post-dates the tilting. The tilting itself has not been directly dated but by analogy with the rapid subsidence of the Lavanttal and west Styrian basins between 18

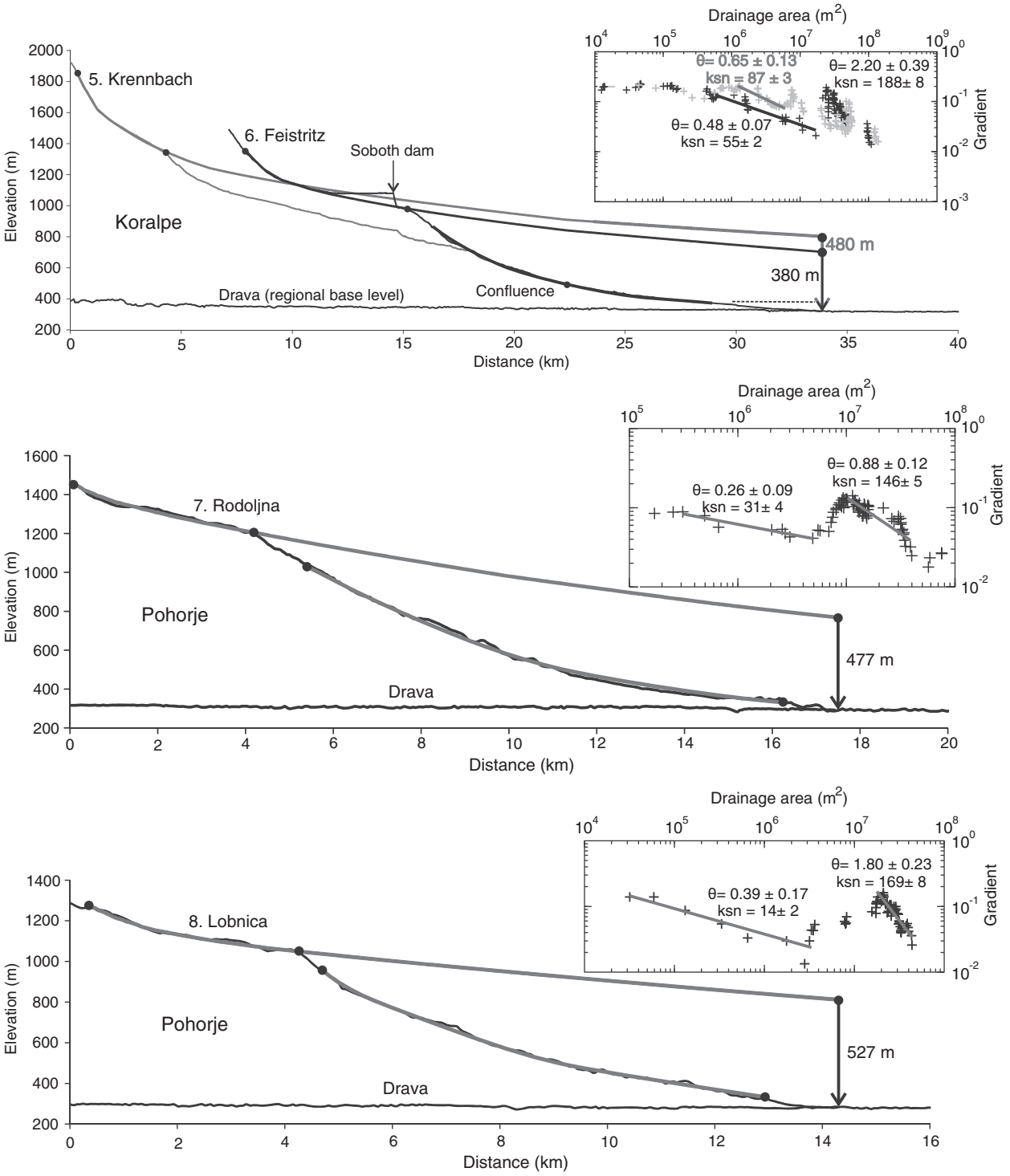

Fig. 7. Channel profile projection for the 4 selected channels of Koralpe and Pohorje draining to the Drava river. For the location of the channels refer to Fig. 3. Thin black lines are the raw and the smoothed channel profiles, thick gray lines are the fitted segments; k = knickpoint; horizontal dashed line on the Koralpe river plot is the top of a fill fluvial terrace of the Drava river from the LGM. For detailed method and parameters used for the slope-area plots refer to Table 1.

and 16 Ma, the tilting of Koralpe is likely to have occurred in this period (Neubauer and Genser, 1990). This indirect time constraint on the formation of the Koralpe relict landscape suggests that the Koralpe relict landscape was formed after ~16 Ma.

Taken together, both the Pohorje and Koralpe relict landscape seem to post-date the very active 18 Ma to 15 Ma period, during the main activity of the lateral extrusion of the eastern Alps. As a consequence, the Koralpe and Pohorje relict landscape probably do not represent pre-Miocene dissected and deformed relict landscapes but a period of quiescence at a later stage. While it seems clear that the relict landscapes are younger than about 15 Ma, the exact timing of their formation and later incision cannot be resolved by our results. Nevertheless, subsidence analysis of adjacent basins can give some constraints on the landscape and uplift evolution for the missing time span since 15 Ma. We have selected subsidence curves from two wells (Fig. 9d, Ebner and Sachsenhofer, 1995; Sachsenhofer et al., 1998, 2001) that have recorded

Table 1
Channel profile analysis for the eight selected rivers. All fitted channels were smoothed with a 500 m moving window and a vertical sampling interval of 15 m was used.

ID	Name	A_{min}[a] (m^2)	A_{max}[a] (m^2)	θ	±2σ	k_s	±2σ	k_{sn}[b]	±2σ	r^2	I[c](m)	±2σ
Relict												
1	Waldensteinerbach	3.40E+05	3.20E+07	0.55	0.05	2.28E+02	9.91E+00	46	2	0.71	241	22
2	Fallegbach	6.00E+05	5.80E+06	0.69	0.11	1.59E+03	1.30E+02	49	4	0.90	403	67
3	Frassbach	2.50E+05	2.60E+07	0.43	0.03	6.60E+01	1.39E+00	95	2	0.94	216	15
4	Schwarze Sulm	5.20E+06	1.80E+07	0.89	0.18	1.14E+05	6.13E+03	93	5	0.87	372	76
5	Krennbach	1.20E+06	6.30E+06	0.65	0.13	1.96E+03	6.76E+01	87	3	0.86	480	97
6	Feistritz	5.80E+05	2.40E+07	0.48	0.07	8.70E+01	3.16E+00	55	2	0.91	380	56
7	Rodoljna	3.00E+05	5.10E+06	0.26	0.09	2.21E+00	2.85E−01	31	4	0.89	477	173
8	Lobnica	2.20E+04	3.40E+06	0.39	0.17	8.25E+00	1.18E+00	14	2	0.80	527	240
											387	**105**
Knickzone												
1	Waldensteinerbach	–	–	–	–	–	–	–	–	–		
2	Fallegbach	6.30E+06	1.10E+07	3.50	0.49	1.03E+23	5.72E+21	162	9	0.84		
3	Frassbach	2.90E+07	3.60E+07	3.90	0.75	4.29E+33	3.02E+32	270	19	0.85		
4	Schwarze Sulm	2.00E+07	6.70E+07	0.86	0.17	2.00E+05	2.88E+03	139	2	0.68		
5	Krennbach	–	–	–	–	–	–	–	–	–		
6	Feistritz	3.40E+07	7.20E+07	2.20	0.39	6.75E+15	2.87E+14	188	8	0.77		
7	Rodoljna	9.50E+06	6.30E+07	0.88	0.12	2.01E+05	6.88E+03	146	5	0.82		
8	Lobnica	1.90E+07	6.00E+07	1.80	0.23	6.18E+12	2.93E+11	169	8	0.85		

Bold number is the mean incision amount for all channels, with standard deviation around the mean.
[a] *Amin* and Amax are the minimum and maximum drainage areas, respectively, used for the fit.
[b] k_{sn} was calculated with a reference concavity index of 0.45.
[c] *I* refers to the calculated incision in m.

vertical movements for the last 18 Ma and are located in the vicinity of Koralpe and Pohorje, in the southern part of the eastern Styrian basin (see Fig. 1 for location of the wells). These subsidence curves as well as other data sets have been interpreted in detail by Ebner and Sachsenhofer (1995) and Sachsenhofer et al. (1998, 2001) and we compare them below with our analysis of the relict landscapes.

The two subsidence curves for the Somat1 and Pichla1 wells (Fig. 9d) indicate that this part of the Styrian basin started to subside

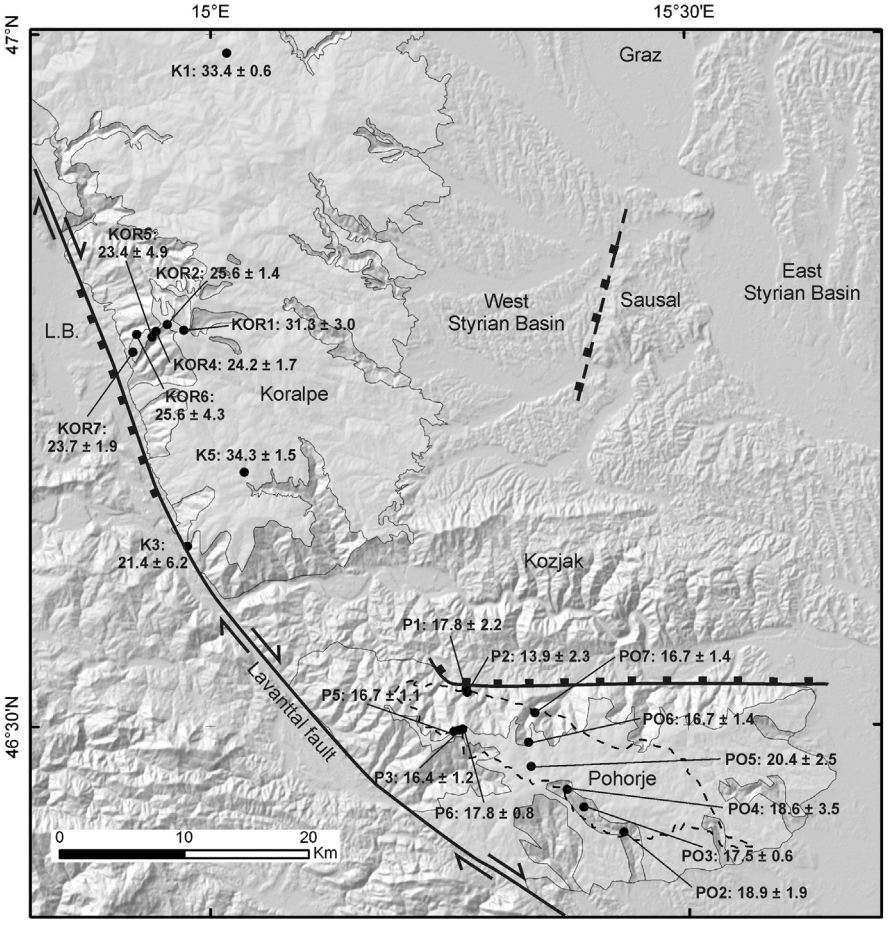

Fig. 8. Results of apatite (U–Th)/He thermochronology. Ages are in Ma ± 1σ. White polygons are the mapped relict landscapes; dashed black line is the boundary of the Pohorje granite.

Table 2
Analytical results for the apatite (U–Th)/He ages with calculated single grains and mean ages.
For location and elevation of the samples refer to Table 3.

Sample	4-He (mol)	238-U (mol)	232-Th (mol)	147-Sm (mol)	Age (Ma)	Uncorr.		Alpha-corr. mean	
						Ft	Age (Ma)	Age (Ma)	±1σ
Pohorje									
PO2 #1	1.75E−14	9.57E−13	1.18E−13	5.72E−13	13.7	0.78	17.5	18.9	1.9
#2	8.98E−15	4.18E−13	1.22E−13	2.78E−13	15.5	0.77	20.2		
PO3 #1	6.10E−15	3.76E−13	6.09E−14	6.22E−14	12.1	0.71	17.1	17.5	0.6
#2	5.14E−15	2.28E−13	3.08E−13	2.77E−13	13.3	0.74	18.0		
PO4 #1	3.92E−15	2.12E−13	1.82E−13	3.11E−13	11.9	0.77	15.3	18.6	3.5
#2	2.67E−15	1.42E−13	1.01E−13	1.34E−13	12.5	0.69	18.2		
#3	1.04E−14	4.54E−13	1.66E−13	2.39E−13	16.4	0.73	22.3		
PO5 #1	7.93E−15	3.44E−13	3.86E−13	5.10E−13	14.1	0.79	17.9	20.4	2.5
#2	6.94E−15	2.69E−13	2.12E−13	3.12E−13	16.8	0.74	22.9		
#3	1.27E−14	5.57E−13	2.53E−13	1.08E−12	15.9	0.78	20.5		
PO6 #1	8.79E−15	4.38E−13	2.33E−13	2.28E−13	13.8	0.76	18.3	16.7	1.4
#2	2.75E−15	1.54E−13	6.71E−14	2.25E−13	12.5	0.78	16.1		
#3	9.35E−15	4.93E−13	3.27E−13	6.35E−13	12.7	0.81	15.7		
PO7 #1	2.95E−15	1.62E−13	1.68E−13	3.19E−13	11.3	0.72	15.7	16.7	1.4
#2	5.53E−15	2.35E−13	3.74E−13	4.08E−13	13.3	0.75	17.7		
P1 #1	3.06E−15	1.23E−13	2.24E−13	2.93E−13	13.5	0.71	19.1	17.8	2.2
#2	2.94E−15	1.60E−13	2.04E−13	2.86E−13	10.9	0.72	15.3		
#3	1.36E−15	6.52E−14	6.97E−14	1.27E−13	12.8	0.67	19.1		
P2 #1	3.98E−15	2.49E−13	1.04E−13	4.30E−13	11.2	0.68	16.4	13.9	2.3
#2	2.43E−15	1.84E−13	1.29E−13	2.24E−13	8.8	0.74	11.8		
#3	8.26E−15	5.54E−13	1.17E−13	1.39E−13	11.0	0.81	13.6		
P3 #1	5.95E−15	3.50E−13	1.57E−13	4.19E−13	11.9	0.77	15.4	16.4	1.2
#2	4.26E−14	2.04E−12	6.50E−13	1.59E−12	15.0	0.85	17.7		
#3	6.11E−15	3.31E−13	2.06E−13	3.81E−13	12.4	0.78	16.0		
P5 #1	9.31E−15	4.71E−13	2.41E−13	5.91E−13	13.6	0.76	18.0	16.7	1.1
#2	2.55E−14	1.35E−12	8.19E−13	1.82E−12	12.8	0.80	16.0		
#3	6.20E−15	3.56E−13	1.74E−13	4.41E−13	12.0	0.75	16.1		
P6 #1	8.93E−15	4.59E−13	2.62E−13	4.75E−13	13.3	0.77	17.3	17.8	0.8
#2	3.77E−15	1.82E−13	1.59E−13	2.52E−13	13.3	0.73	18.3		
Koralpe									
K1 #1	1.12E−14	3.16E−13	4.33E−14	1.83E−12	25.9	0.78	33.1	33.4	0.6
#2	2.47E−14	6.69E−13	9.36E−14	1.80E−12	27.3	0.83	33.0		
#3	1.16E−14	3.23E−13	3.59E−14	1.55E−12	26.4	0.77	34.1		
K3 #1	2.74E−15	8.49E−14	4.17E−14	1.20E−13	22.3	0.79	28.1	21.4	6.2
#2	1.76E−15	9.96E−14	1.38E−14	1.54E−13	13.1	0.82	16.0		
#3	1.34E−15	6.54E−14	1.57E−14	9.76E−14	14.9	0.74	20.2		
K5 #1	1.08E−14	3.01E−13	2.48E−14	1.02E−13	27.0	0.81	33.2	34.3	1.5
#2	3.48E−15	8.60E−14	2.04E−14	2.15E−13	29.3	0.83	35.4		
KOR1 #1	6.65E−14	1.93E−12	1.78E−13	2.64E−13	26.0	0.86	30.2	31.3	3.0
#2	1.19E−14	3.14E−13	1.60E−14	1.49E−13	28.8	0.83	34.7		
#3	2.33E−14	7.37E−13	5.84E−14	8.40E−14	24.0	0.82	29.1		
KOR2 #1	1.04E−14	3.65E−13	5.25E−14	6.56E−13	21.1	0.78	26.9	25.6	1.4
#2	8.30E−15	3.26E−13	6.97E−14	5.17E−13	18.6	0.77	24.2		
#3	1.78E−14	6.30E−13	8.38E−14	1.13E−12	20.9	0.81	25.8		
KOR4 #1	2.45E−15	9.86E−14	5.69E−15	2.74E−14	18.9	0.81	23.4	24.2	1.7
#2	5.11E−15	1.87E−13	1.86E−14	2.94E−14	20.6	0.79	26.1		
#3	3.36E−15	1.35E−13	8.47E−15	3.17E−14	18.9	0.82	23.1		
KOR5 #1	1.26E−14	4.48E−13	1.91E−14	4.30E−13	21.5	0.80	26.9	23.4	4.9
#2	4.29E−15	2.04E−13	4.51E−14	1.11E−13	15.5	0.77	20.0		
KOR6 #1	5.88E−15	1.80E−13	3.11E−14	5.20E−13	24.0	0.77	30.9	25.6	4.3
#2	6.18E−15	2.45E−13	2.32E−14	5.61E−13	18.9	0.78	24.3		
#3	6.24E−15	2.26E−13	2.67E−14	6.41E−13	20.5	0.77	26.5		
#4	4.76E−16	2.03E−14	7.25E−15	5.23E−14	16.6	0.80	20.7		
KOR7 #1	5.01E−15	2.16E−13	8.28E−14	4.08E−13	16.3	0.76	21.4	23.7	1.9
#2	5.85E−15	2.39E−13	5.87E−14	4.73E−13	17.7	0.76	23.3		
#3	4.12E−14	1.25E−12	8.74E−13	1.84E−12	21.8	0.84	26.0		
#4	5.76E−15	2.22E−13	7.57E−14	3.94E−13	18.5	0.76	24.3		

very quickly between 18 Ma and 16 Ma. From 16 to 12 Ma, the subsidence was slower and was eventually followed by a quiet period from 12 to 5 Ma. Around 6–5 Ma, the basins began to invert and started to uplift. This situation prevailed until the present. The estimated amount of uplift since the inversion of the basins from subsidence analysis of these two wells is 400–600 m (Ebner and Sachsenhofer, 1995; Sachsenhofer et al., 1998, 2001). This amount of uplift matches well with the amount of incision that we have calculated from channel profile projection of the channels (387 ± 105 m). This inversion of the basins and associated increased rock uplift rate in the whole area can explain the documented incision into the relict landscape. Thus, even though the incision into the relict landscapes could not be dated directly, it is tempting to suggest that the described incision and the uplift of the basin are the result of the same mechanism. Another interesting comparison is possible with the incision of the Mur river north of Graz, which incised at a rate of approximately 100 m/my for the last 4 Ma, as inferred from cave sediment burial age dating (Wagner et al., 2010). If the uplift and incision did start around 5 or 6 Ma, as suggested

Table 3
Results of the apatite (U–Th)/He ages measured in this study with geographic coordinates and elevation of the samples. Coordinates are in decimal degrees (WGS84).

Sample	Longitude	Latitude	Elevation (m)
Pohorje			
PO2	15.432	46.423	637
PO3	15.390	46.442	887
PO4	15.373	46.454	1042
PO 5	15.335	46.471	1297
PO6	15.333	46.489	1211
PO7	15.340	46.510	966
P1	15.268	46.528	746
P2	15.269	46.525	840
P3	15.260	46.498	1409
P5	15.255	46.497	1517
P6	15.264	46.498	1437
Koralpe			
K1	15.017	46.987	791
K3	14.976	46.631	823
K5	15.035	46.684	1076
KOR1	14.972	46.787	2140
KOR2	14.955	46.791	1949
KOR4	14.943	46.786	1603
KOR5	14.938	46.782	1467
KOR6	14.922	46.784	1273
KOR7	14.919	46.771	1015

by subsidence analysis, the resulting amount of incision should be comprised between 500 m and 600 m. This is of the same order of magnitude as what we have calculated here (387 ± 105 m).

It is suggested that the following scenario from the early Miocene to the present occurred: during the early Miocene faulting, deformation and uplift of the Koralpe and Pohorje mountains occurred (Fig. 10). During the quiet middle Miocene period we suggest that the relict landscape was formed. Potentially more rugged topography from the early Miocene was smoothed and lowered at this time. During this time, the Drava river behaved antecedently so that we interpret it to have remained at constant elevation throughout the timescale under discussion. The rivers connected to the Drava started to incise and record the surface uplift of Koralpe and Pohorje (Figs. 10, 11). Then, the Koralpe and Pohorje mountains, as well as the surrounding sedimentary basins were uplifted together for some 400 m in a renewed uplift event that started at the end of Miocene.

This interpretation partly contradicts previous work and we explain in the following why we think that our interpretation is more consistent with the observations. For example, Frisch et al. (2000) interpreted the Koralpe paleosurface to be of Oligocene age. This is contradicted by the morphometric analysis and in particular by the fact that the Koralpe relict landscape is symmetric to the range, regardless of the Miocene tilting. Our results also contradict the idea of a surface uplift of the Koralpe range of more than 800 m since the late Miocene, as it has been suggested based on occurrence of gravels on top of the Koralpe

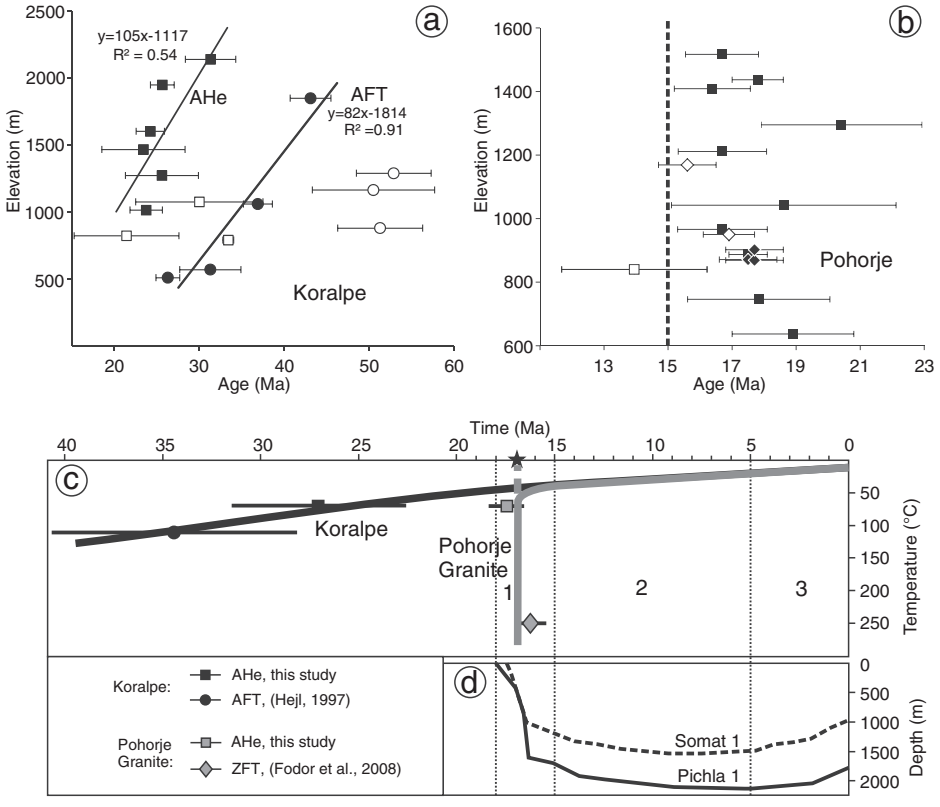

Fig. 9. Age–elevation relationship of thermochronology data and cooling paths of the Koralpe and Pohorje mountains. (a) Age–elevation relationship of Koralpe. Squares are apatite (U–Th)/He ages (this study); black squares are the samples of the profile taken from the western slope of Koralpe (samples KOR1 to KOR7) that are included for the linear regression (black line); white squares are the samples located in other parts of Koralpe. Circles are apatite fission track ages (Hejl, 1997); Black circles are included in the linear regression and white circles are from other locations in Koralpe (see Hejl (1997) for location of the samples and details of the linear regression). (b) Age–elevation relationship of Pohorje. Squares are apatite (U–Th)/He ages (this study); black squares are granitic samples and the white square is the volcanic rock sample (P2); Diamonds are ZFT ages (Fodor et al., 2008); Black diamonds are granitic samples and white diamonds are volcanic rock samples (dacite). See Fodor et al. (2008) for the location of the ZFT samples. Vertical dashed line represents the youngest apatite (U–Th)/He age from the granitic samples considering error bars (15 Ma). (c) Cooling path for Koralpe and Pohorje based on the different thermochronological ages. Symbols are the mean ages for the entire area with error bars representing the standard deviation around the mean. Thick lines are inferred cooling paths for Koralpe and Pohorje. The black star refers to the oldest known sediments where magmatic pebbles have been found (Fodor et al., 2008); thick dashed gray line indicate exhumation of the part of Pohorje granite to the surface. Vertical lines and numbers refer to the different periods discussed in the text for the interpretation of the tectonic and landscape evolution of the area. (d) Subsidence curves of two wells (Somat 1, Pichla 1) of the Styrian basins (Ebner and Sachsenhofer, 1995; Sachsenhofer et al., 1998, 2001); see Fig. 1 for the location of the wells.

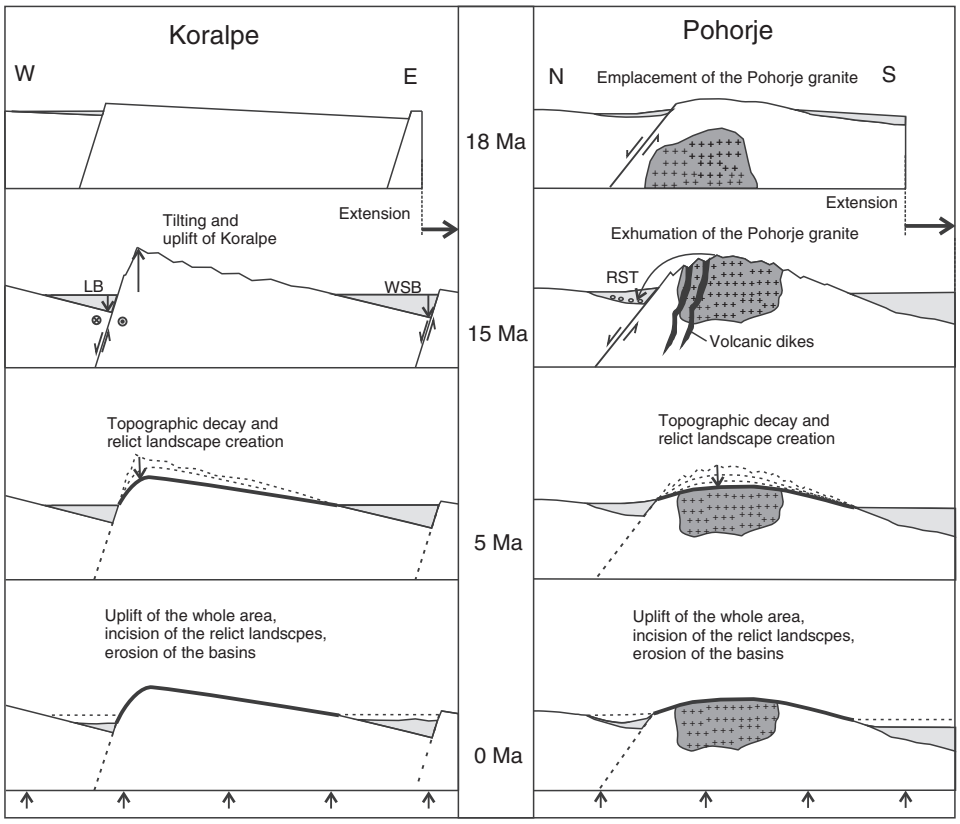

Fig. 10. Inferred scenario for the landscape and tectonic evolution of the studied area since the early Miocene. Schematic cross-section of Koralpe and Pohorje (not to scale) with different time steps depicting tectonic processes and landscape evolution.

paleosurface (Pischinger et al., 2008; Kurz et al., 2011). However, gravels occur in elevated positions throughout the eastern end of the Alps where they are referred to as the Augenstein surface and little is known about their deposition age, which could potentially be much older (e.g. Frisch et al., 2001). We rather suggest a surface uplift event of around 400 m based on the channel profile analysis and suggest a 5 Ma time frame for this uplift. We believe that this is a more robust estimate given the fact that this is based on the analysis of eight channels over a larger area. Our results also clearly contradict the interpretation that the Koralpe rivers are well-equilibrated and do not feature significant knickpoints other than lithological (Rantitsch et al., 2009). Despite the contradictions listed above a significant part of our interpretations does in fact support previous work. Our results are in line with the following interpretation: (1) most of the Koralpe landscape is a relict landscape (Winkler-Hermaden, 1957; Frisch et al., 2000), (2) the Koralpe range can be considered as an eastward tilted block (Genser and Neubauer, 1989; Frisch et al., 2000; Kurz et al., 2011), and (3) the exhumation of the Pohorje granite was extremely fast and related to tectonic denudation due to the early Miocene extension (Sachsenhofer et al., 1998; Fodor et al., 2008).

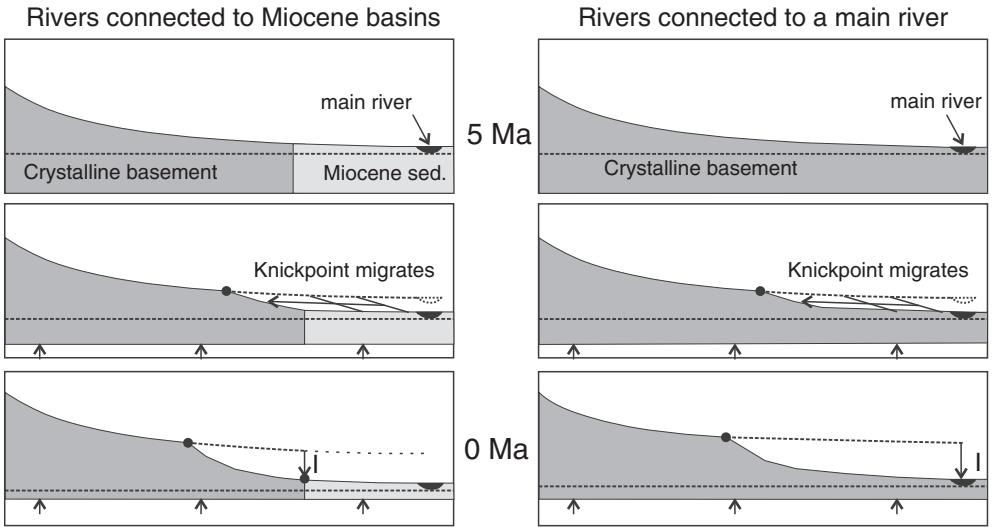

Fig. 11. Schematic channel profiles through different time steps during the incision into the Koralpe and Pohorje relict landscapes. I refers to Incision amount.

The implication of our interpretation for the landscape evolution elsewhere in the eastern Alps and beyond is profound. General consensus holds that uplift and land forming processes in much of the Alps have either come to a halt (Willett et al., 2006) or that this uplift is driven by glacial erosion of the last million years (e.g. Champagnac et al., 2007; Willett, 2010; Sternai et al., 2012). The sedimentation rates of Kuhlemann et al. (2002) have partly been used in support of these ideas. However, it has recently been noted that the onset of rapid sedimentation around the Alps as documented by Kuhlemann et al. (2002) is somewhat earlier than the onset of glaciation and that this hiatus remains unexplained. Here, we present further evidence for a young uplift event that coincides with the increase of sedimentation rates around the Alps and is clearly unrelated to glaciation. In fact it rather relates – at least temporally – to what has been termed a basin inversion event for the Pannonian basin (Peresson and Decker, 1997; Bada et al., 2007; Wagner et al., 2010, 2011). Although we have documented this tectonically-driven uplift event only in the eastern end of the Alps, we argue here that it is possible that many observations further west are related to this event. In particular, we highlight this possibility for observations of observed hanging valleys, incised gorges or elevated planation surfaces elsewhere in the Alps that indicate some hundreds of meters of relative uplift. In this context, we suggest that tectonically driven uplift events of the last 5 Ma may have assisted the formation of the Alpine ice cap during the subsequent glaciation periods and argue therefore ultimately for tectonic drivers for the land forming processes.

6. Conclusion

Several conclusions are drawn concerning the landscape evolution of the Koralpe and Pohorje mountains: 1.) The Koralpe and Pohorje mountains show strong evidence of transient erosion based on hillslopes and channel profile analysis. Their landscapes can be divided in an upper relict landscape, and lower incised landscape. 2.) The Koralpe and Pohorje relict landscapes are younger than 16–15 Ma, as indicated by the exhumation of the Pohorje granite and the extent of the relict landscape on both sides of the tilted Koralpe block. 3.). The incision into the two relict landscapes averages 383 m $\pm$ 105 m and is probably the result of an increased rock uplift rate since the latest Miocene (6–5 Ma) affecting the studied mountains and the surrounding Miocene basins. 4.) The Koralpe and Pohorje relict landscapes were most likely created during the late Miocene, between 16–15 Ma and 5 Ma, a period of tectonic quiescence that allowed the topography to decay and become smoother. 5.) Finally, we emphasize that the documented young uplift event is older than the glaciation periods and suggest that observations elsewhere in the Alps may therefore have been mistakenly interpreted as evidence for glacial erosion. Moreover, we suggest that this uplift event may have assisted in the formation of the Alpine ice cap during the glaciation periods and argue therefore ultimately for a tectonic driver for the land forming processes in the Alps.

Acknowledgments

This work was funded by ESF/FWF Topo-Alps project (I152-N19). We are grateful to Todd Ehlers and Eva Enkelmann for their help with the laboratory work for the geochronology and interesting discussions. We thank Wolfgang Frisch, Kevin Norton, Eva Enkelmann and an anonymous reviewer for their reviews of earlier versions of this manuscript. Finally, we would like to thank our editor Andy Plater for considerate handling of this manuscript.

References

Bada, G., Horvath, F., Dövenyi, P., Szafian, P., Windhoffer, G., Cloetingh, S., 2007. Present-day stress field and tectonic inversion in the Pannonian basin. Glob. Planet. Chang. 58, 165–180.

Cederbom, C.E., Sinclair, D.H., Schlunegger, F., Meinert, K.R., 2004. Climate-induced rebound and exhumation of the European Alps. Geology 32, 709–712. http://dx.doi.org/10.1130/G20491.1.

Champagnac, J.D., Molnar, P., Anderson, R.S., Sue, C., Delacou, B., 2007. Quaternary erosion-induced isostatic rebound and exhumation of the European Alps. Geology 35, 195–198. http://dx.doi.org/10.1130/G23053A.1.

Clark, M.K., Maheo, G., Saleeby, J., Farley, K.A., 2005. The non-equilibrium landscape of the southern Sierra Nevada, California. GSA Today 15. http://dx.doi.org/10.1130/1052-5173(2005)015<4:TNELOT>2.0.CO;2.

Clark, M.K., Royden, L.H., Whipple, K.X., Burchfiel, B.C., Zhang, X., Tang, W., 2006. Use of a regional, relict landscape to measure vertical deformation of the eastern Tibetan Plateau. J. Geophys. Res. 111, F03002. http://dx.doi.org/10.1029/2005JF000294.

Dunkl, I., Kuhlemann, J., Reinecker, J., Frisch, W., 2005. Cenozoic relief evolution of the Eastern Alps — constraints from apatite fission track age-provenance of Neogene intramontane sediments. Austrian J. Earth Sci. 98, 92–105.

Ebner, E., Sachsenhofer, R.E., 1995. Paleogeography, subsidence and thermal history of the Neogene Styrian Basin (Pannonian basin system, Austria). In: Neubauer, E., Ebner, E., Wallbrecher, E. (Eds.), Tectonics of the Alpine–Carpathian–Pannonian Region. Tectonophysics, 242, pp. 133–150.

Ehlers, T.A., Farley, K.A., 2003. Apatite (U–Th)/He thermochronometry: methods and applications to problems in tectonic and surface processes. Earth Planet. Sci. Lett. 206, 1–14.

Exner, C., 1976. Die geologische Position der Magmatite des periadriatischen Lineamentes. Verh. Geol. B.-A. 1976 (2), 3–64.

Farley, K., 2000. Helium diffusion from apatite; general behavior as illustrated by Durango fluorapatite. J. Geophys. Res. 105, 2903–2914. http://dx.doi.org/10.1029/1999JB900348.

Flint, J.J., 1974. Stream gradient as a function of order, magnitude, and discharge. Water Resour. Res. 10, 969–973.

Fodor, L., Gerdes, A., Dunkl, I., Koroknai, B., Pecskay, Z., Trajanova, M., Horvath, P., Vrabec, M., Jelen, B., Balogh, K., Frisch, W., 2008. Miocene emplacement and rapid cooling of the Pohorje pluton at the Alpine–Pannonian–Dinaridic junction, Slovenia. Swiss J. Geosci. 101, 255–271.

Frisch, W., Kuhlemann, J., Dunkl, I., Brügel, A., 1998. Palinpastic reconstruction and topographic evolution of the Eastern Alps during the late Tertiary extrusion. Tectonophysics 297, 1–15.

Frisch, W., Dunkl, I., Kuhlemann, J., 2000. Post-collisional largescale extension in the Eastern Alps. Tectonophysics 327, 239–265.

Frisch, W., Kuhlemann, J., Dunkl, I., Szekely, B., 2001. The Dachstein paleosurface and the Augenstein Formation in the Northern Calcareous Alps; a mosaic stone in the geomorphological evolution of the Eastern Alps. Int. J. Earth Sci. 90, 500–518.

Genser, J., Neubauer, F., 1989. Low angle normal faults at the eastern margin of the Tauern window (Eastern Alps). Mitteilungen der Österreichischen Geologischen Gesellschaft 81, 233–243.

Hack, J.T., 1973. Stream-profile analysis and stream-gradient index. J. Res. U. S. Geol. Surv. 1, 421–429.

Hejl, E., 1997. "Cold spots" during the Cenozoic evolution of the Eastern Alps: thermochronological interpretation of apatite fission-track data. Tectonophysics 272, 159–173.

Hergarten, S., Wagner, T., Stüwe, K., 2010. Age and prematurity of the Alps derived from topography. Earth Planet. Sci. Lett. 297, 453–460.

Hirt, C., Filmer, M.S., Featherstone, W.E., 2010. Comparison and validation of the recent freely available ASTER-GDEM ver1, SRTM ver4.1 and GEODATA DEM-9S ver3 digital elevation models over Australia. Aust. J. Earth Sci. 57, 337–347.

Kuhlemann, J., Frisch, W., Szekely, B., Dunkl, I., Kazmer, M., 2002. Postcollisional sediment budget history of the Alps: tectonic versus climatic control. Int. J. Earth Sci. 91, 818–837.

Kurz, W., Wölfler, A., Rabitsch, R., Genser, J., 2011. Polyphase movement on the Lavanttal Fault Zone (Eastern Alps): reconciling the evidence from different geochronological indicators. Swiss J. Geosci. 104, 323–343. http://dx.doi.org/10.1007/s00015-011-0068-y.

McDowell, F.W., McIntosh, W.C., Farley, K.A., 2005. A precise 40Ar–39Ar reference age for the Durango apatite (U–Th)/He and fission-track dating standard. Chem. Geol. 214, 249–263.

Neubauer, F., Genser, J., 1990. Architektur und Kinematik der östlichen Zentralalpen – eine Übersicht. Mitt. Naturwiss. Ver. Steiermark 120, 203–219.

Norton, K.P., Abbühl, L.M., Schlunegger, F., 2010. Glacial conditioning as an erosional driving force in the Central Alps. Geology 38, 655–658. http://dx.doi.org/10.1130/G31102.1.

Peresson, H., Decker, K., 1997. Far-field effects of Late Miocene subduction in the Eastern Carpathians: E–W compression and inversion of structures in the Alpine–Carpathian–Pannonian region. Tectonics 16, 38–56. http://dx.doi.org/10.1029/96TC02730.

Persaud, M., Pfiffner, O.A., 2004. Active deformation in the eastern Swiss Alps: post-glacial faults, seismicity and surface uplift. Tectonophysics 385, 59–84. http://dx.doi.org/10.1016/j.tecto.2004.04.020.

Pischinger, G., Kurz, W., Übleis, M., Egger, M., Fritz, H., Brosch, F.J., Stingl, K., 2008. Fault slip analysis in the Koralm Massif (Eastern Alps) and consequences for the final uplift of "cold spots" in Miocene times. Swiss J. Geosci. 101, 235–254.

Rantitsch, G., Pischinger, G., Kurz, W., 2009. Stream profile analysis of the Koralm Range (Eastern Alps). Swiss J. Geosci. 102, 31–41.

Ratschbacher, L., Frisch, W., Linzer, H.G., Merle, O., 1991. Lateral extrusion in the Eastern Alps, Part 2. Structural analysis. Tectonics 10, 257–271.

Reinecker, J., Lenhardt, W.A., 1999. Present-day stress field and deformation in eastern Austria. Int. J. Earth Sci. 88, 532–550.

Reischenbacher, D., Rifelj, H., Sachsenhofer, R.F., Jelen, B., Coric, S., Gross, M., Reichenbacher, B., 2007. Early Badenian paleoenvironment in the Lavanttal Basin

(Mühldorf Formation; Austria): evidence from geochemistry and Paleontology. Austrian J. Earth Sci. 100, 202–229.
Robl, J., Stüwe, K., 2005. Continental collision with finite indenter strength: 2. European Eastern Alps. Tectonics 24. http://dx.doi.org/10.1029/2004TC001741.
Robl, J., Hergarten, S., Stüwe, K., 2008. Morphological analysis of the drainage system in the Eastern Alps. Tectonophysics 460, 263–277.
Sachsenhofer, R.F., Lankreijer, A., Cloetingh, S., Ebner, F., 1997. Subsidence analysis and quantitative basin modeling in the Styrian basin (Pannonian Basin system, Austria). Tectonophysics 272, 175–196.
Sachsenhofer, R.F., Dunkl, I., Hasenhüttl, C., Jelen, B., 1998. Miocene thermal history of the southwestern margin of the Styrian Basin: vitrinite reflectance and fission-track data from the Pohorje/Kozjak area (Slovenia). Tectonophysics 297, 17–29.
Sachsenhofer, R.F., Jelen, B., Hasenhüttl, C., Dunkl, I., Rainer, T., 2001. Thermal history of Tertiary basins in Slovenia (Alpine–Dinaride–Pannonian junction). Tectonophysics 334, 77–99.
Schoenbohm, L.M., Whipple, K.X., Burchfiel, B.C., Chen, L., 2004. Geomorphic constraints on surface uplift, exhumation, and plateau growth in the Red River region, Yunnan Province, China. GSA Bull. 116, 895–909. http://dx.doi.org/10.1130/B25364.1.
Shuster, D.L., Flowers, R.M., Farley, K.A., 2006. The influence of natural radiation damage on helium diffusion kinetics in apatite. Earth Planet. Sci. Lett. 249, 148–161.
Sölva, H., Stüwe, K., Strauss, P., 2005. The Drava River and the Pohorje Mountain range (Slovenia): geomorphological interactions. Mitt. Naturwiss. Ver. Steiermark 134, 45–55.
Sternai, P., Herman, F., Champagnac, J.D., Fox, M.R., Salcher, B., Willett, S.D., 2012. Pre-glacial topography of the European Alps. Geology 40, 1067–1070. http://dx.doi.org/10.1130/G33540.1.
Strauss, P., Wagreich, M., Decker, K., Sachsenofer, R.F., 2001. Tectonics and sedimentation in the Fohnsdorf-Seckau Basin (Miocene, Austria): from a pull-apart basin to a half-graben. Int. J. Earth Sci. 90, 549–559.
Valla, P.G., Schuster, D.L., van der Beek, P., 2011. Significant increase in relief of the European Alps during mid-Pleistocene glaciations. Nat. Geosci. 4, 688–692. http://dx.doi.org/10.1038/ngeo1242.
van Husen, D., 1997. LGM and late-glacial fluctuations in the Eastern Alps. Quat. Int. 38/39, 109–118.
Wagner, T., Fabel, D., Fiebig, M., Häuselmann, P., Sahy, D., Xu, S., Stüwe, K., 2010. Young uplift in the non-glaciated parts of the Eastern Alps. Earth Planet. Sci. Lett. 295, 159–169.
Wagner, T., Fritz, H., Stüwe, K., Nestroy, O., Rodnight, H., Hellstrom, J., Benischke, R., 2011. Correlations of cave levels, stream terraces and planation surfaces along the River Mur — timing of landscape evolution along the eastern margin of the Alps. Geomorphology 295, 159–169. http://dx.doi.org/10.1016/j.geomorph.2011.04.024.
Whipple, K.X., Wobus, C., Crosby, B., Kirby, E., Sheehan, D., 2007. Stream profiler tool. www.geomorphtools.org.
Willett, S.D., 2010. Late Neogene erosion of the Alps: a climate driver? Annu. Rev. Earth Planet. Sci. 38, 411–437.
Willett, S.D., Schlunegger, F., Picotti, V.I., 2006. Messinian climate change and erosional destruction of the Central European Alps. Geology 34, 613–616.
Winkler-Hermaden, A., 1957. Geologisches Kräftespiel und Landformung. Springer Verlag, Vienna, (822 pp.).
Wobus, C., Whipple, K.X., Kirby, E., Snyder, N., Johnson, J., Spyropolou, K., Crosby, B., Sheehan, D., 2006. Tectonics from topography: procedures, promise, and pitfalls. GSA Spec. Pap. 398, 55–74.
Wolf, R.A., Farley, K.A., Kass, D.M., 1998. Modeling of the temperature sensitivity of the apatite (U–Th)/He thermochronometer. Chem. Geol. 148, 105–114.
Wölfler, A., Kurz, W., Danisik, M., Rabitsch, R., 2010. Dating of fault zone activity by apatite fission track and apatite (U–Th)/He thermochronometry: a case study from the Lavanttal fault system (Eastern Alps). Terra Nova 22, 274–282. http://dx.doi.org/10.1111/j.13653121.2010.00943.x.
Wölfler, A., Kurz, W., Fritz, H., Stüwe, K., 2011. Lateral extrusion in the Eastern Alps revisited: refining the model by thermochronological, sedimentary and seismic data. Tectonics 30, TC4006. http://dx.doi.org/10.1029/2010TC002782.